

# Constraints on Cosmological Parameters from the Analysis of the Cosmic Lens All Sky Survey Radio-Selected Gravitational Lens Statistics

K.-H. Chae,<sup>1</sup> A.D. Biggs,<sup>1</sup> R.D. Blandford,<sup>2</sup> I.W.A. Browne,<sup>1</sup> A.G. de Bruyn,<sup>3</sup>  
C.D. Fassnacht,<sup>4</sup> P. Helbig,<sup>1</sup> N.J. Jackson,<sup>1</sup> L.J. King,<sup>5</sup> L.V.E. Koopmans,<sup>2</sup> S. Mao,<sup>1</sup>  
D.R. Marlow,<sup>6</sup> J.P. McKean,<sup>1</sup> S.T. Myers,<sup>7</sup> M. Norbury,<sup>1</sup> T.J. Pearson,<sup>2</sup> P.M. Phillips,<sup>1</sup>  
A.C.S. Readhead,<sup>2</sup> D. Rusin,<sup>8</sup> C.M. Sykes,<sup>1</sup> P.N. Wilkinson,<sup>1</sup> E. Xanthopoulos,<sup>1</sup> and T. York<sup>1</sup>

<sup>1</sup>*University of Manchester, Jodrell Bank Observatory, Macclesfield, Cheshire, SK11 9DL, UK*

<sup>2</sup>*California Institute of Technology, Pasadena, CA 91125*

<sup>3</sup>*NFRA, Postbus 2, 7990 AA Dwingeloo, The Netherlands*

<sup>4</sup>*Space Telescope Science Institute, 3700 San Martin Drive, Baltimore, MD 21218*

<sup>5</sup>*University of Bonn, Auf dem Hugel, 69, D-53121 Bonn, Germany*

<sup>6</sup>*Dept. of Physics and Astronomy, University of Pennsylvania, 209 S. 33rd Street Philadelphia, PA 19104*

<sup>7</sup>*National Radio Astronomy Observatory, P.O. Box 0, Socorro, NM 87801*

<sup>8</sup>*Harvard-Smithsonian Center for Astrophysics, 60 Garden St., MS-51, Cambridge, MA 02138*

(Dated: April 6, 2018)

We derive constraints on cosmological parameters and the properties of the lensing galaxies from gravitational lens statistics based on the final Cosmic Lens All Sky Survey (CLASS) data. For a flat universe with a classical cosmological constant, we find that the present matter fraction of the critical density is  $\Omega_m = 0.31^{+0.27}_{-0.14}$  (68%)  $^{+0.12}_{-0.10}$  (systematic). For a flat universe with a constant equation of state for dark energy  $w = p_x(\text{pressure})/\rho_x(\text{energy density})$ , we find  $w < -0.55^{+0.18}_{-0.11}$  (68%).

PACS numbers: 98.80.-k,98.80.Es,98.80.Cq,98.62.Py

Gravitational lensing, in which a background source behind a foreground object is seen as distorted and (de)magnified image(s), is well-understood by the simple physics of light deflections in a weak gravitational field. Hence, the analysis of lens statistics can provide a technique [1] for constraining cosmological parameters that is both powerful and complementary to other methods [2]. However, for lens statistics to be useful, it is vital to have an unbiased statistical sample of sources that is complete within well-defined observational selection criteria [3] and to properly take into account all factors in a statistical lensing model [4]. The statistical properties of gravitational lensing in a sample are the total lensing rate, the image separations, the lens redshifts, the source redshifts, and the image multiplicities. These properties depend not only on cosmological parameters but also on the properties of the lensing galaxies and the distributions of the sources in redshift ( $z$ ) and in luminosity in the observational selection waveband (e.g. radio here) [4].

Recent advances in observations permit us to do a reliable analysis of lens statistics to obtain limits on cosmological parameters. First, the largest radio-selected galactic mass-scale gravitational lens search project to date, the Cosmic Lens All Sky Survey (CLASS), has now been completed, resulting in the largest sample suitable for statistical analyses [3]. Second, currently available independent data sets on the distributions of (flat spectrum) radio sources in flux density and in redshift are concordant [3, 4]. Third, recent large-scale observations of galaxies, in particular the Two Degree Field Galaxy Redshift Survey (2dFGRS) and the Sloan Digital Sky Survey (SDSS), have produced converging results on the

total galaxy luminosity function (LF; i.e., distribution of galaxy number density in luminosity), and there exist fairly reliable observational results that permit us to extract from the total LF morphological type-specific LFs, i.e., an early-type (i.e. ellipticals and S0 galaxies) LF and a late-type (i.e. spirals and others) LF [4, 5]. In this Letter, we report the main results on cosmological parameters from a likelihood analysis of lens statistics based on these crucial sets of data. The detailed procedure of the analysis will be described in a later publication [4] in which extended analyses will be presented for broader range of parameters and with an emphasis on the global properties of galaxy populations.

The CLASS statistical sample suitable for our analysis contains 8958 radio sources out of which 13 sources are multiply-imaged [3]. The lens search looked for multiple-lensing image components of the central compact radio core in the background sources. The CLASS statistical sample is defined so as to meet the following observational selection criteria [3]: (1) the spectral index between 1.4 GHz and 5 GHz is flatter than  $-0.5$ , i.e.  $\alpha \geq -0.5$  with  $S_\nu \propto \nu^\alpha$  where  $S_\nu$  is flux density measured in milli-jansky (mJy; 1 mJy  $\equiv 10^{-29}$  W m<sup>-2</sup> Hz<sup>-1</sup>); (2) the total flux density of each source is  $\geq 30$  mJy at 5 GHz; (3) the total flux density of each source is  $\geq 20$  mJy at 8.4 GHz; (4) the image components in lens systems must have separations  $\geq 0.3$  arcsec and the ratio of the flux densities of the fainter to the brighter component in double-image systems must be  $\geq 0.1$ . Number counts for sources at  $\nu = 5$  GHz are consistent with a (broken) power-law differential number-flux density relation  $|dN/dS|$  (i.e. number of sources per flux density bin)

TABLE I: Gravitational lens systems in the well-defined CLASS statistical sample.  $z_s$  and  $z_l$  are source and lens redshifts, respectively; for sources with unmeasured redshifts, we take  $z_s = 2$ , which is the mean source redshift for the entire sample of CLASS lenses. The maximum image separation ( $\Delta\theta$ ) is given in arcsec. Image multiplicity is listed under  $N_{\text{im}}$ . When the image splitting is due to multiple galaxies, the image separation and the image multiplicity are not used in our model fitting. The image separation of 2045+265 is not used because of uncertainties in the nature of the lensing scenario. Probable lens galaxy type identification (G-type) is coded as: e for an early-type and s for a spiral-type.

Source	$z_s$	$z_l$	$\Delta\theta$	$N_{\text{im}}$	G-type
0218+357	0.96	0.68	0.334	2	s
0445+123	-	-	1.33	2	-
0631+519	-	-	1.16	2	-
0712+472	1.34	0.41	1.27	4	e
0850+054	-	-	0.68	2	-
1152+199	1.019	0.439	1.56	2	-
1359+154	3.235	-	1.65	6	- (3 Gs)
1422+231	3.62	0.34	1.28	4	e
1608+656	1.39	0.64	2.08	4	e (2 Gs)
1933+503	2.62	0.755	1.17	4	e?
2045+265	-	0.867	1.86	4	-
2114+022	-	0.32/0.59	2.57	2?	e (2 Gs)
2319+051	-	0.624	1.36	2	e

$\propto (S/S^0)^{-\eta}$  with  $\eta = 2.07 \pm 0.02$  ( $1.97 \pm 0.14$ ) for  $S \geq S^0$  ( $S \leq S^0$ ) and  $S^0 = 30$  mJy. These results are consistent with the prediction of the Dunlop & Peacock (1990) free-form model number 5 radio luminosity function that is consistent with redshift data at  $S > 1$  mJy [3, 4]. Redshift measurements for a representative CLASS subsample and the prediction of the aforementioned Dunlop & Peacock (1990) model consistently suggest that the redshift distribution for the CLASS unlensed sources can be adequately described by a Gaussian model with mean redshift,  $\langle z \rangle = 1.27$  and dispersion 0.95 [3, 4]. The properties of the 13 multiply-imaged sources are summarized in Table 1.

The luminosity function of galaxies is assumed to be well-described by a Schechter function [5] of the form

$$\frac{dn}{d(L/L_*)} = n_* \left( \frac{L}{L_*} \right)^\alpha \exp(-L/L_*), \quad (1)$$

where  $\alpha$  is a faint-end slope and  $n_*$  and  $L_*$  are characteristic number density and characteristic luminosity, respectively. From Eq. (1) an integrated luminosity density  $j$  is given by  $j = \int_0^\infty dLL(dn/dL) = n_* L_* \Gamma(\alpha + 2)$ . The luminosity of a galaxy is correlated with its line-of-sight stellar velocity dispersion ( $\sigma$ ) via the empirical relations,

$$\frac{L}{L_*} \equiv 10^{0.4(M_* - M)} = \left( \frac{\sigma}{\sigma_*} \right)^\gamma, \quad (2)$$

where  $M_*$  and  $\sigma_*$  are respectively characteristic absolute magnitude and characteristic velocity disper-

sion, and  $\gamma$  corresponds to the Faber-Jackson (Tully-Fisher) exponent for an early-type (late-type) population [6]; throughout we take  $\gamma_{\text{Faber-Jackson}} = 4.0$  and  $\gamma_{\text{Tully-Fisher}} = 2.9$  [6]. The 2dFGRS team and the SDSS team independently determine the Schechter parameters for galaxies at  $z \lesssim 0.2$  summed over all galactic types and their results are consistent with each other [5]. The converging result can be expressed in the  $b_J$  photometric system as  $M_* - 5 \log_{10} h = -19.69 \pm 0.04$  (hereafter  $h$  is the Hubble constant  $H_0$  in units of  $100 \text{ km s}^{-1} \text{ Mpc}^{-1}$ ),  $\alpha = -1.22 \pm 0.02$ , and  $n_* = (1.71 \pm 0.07) \times 10^{-2} h^3 \text{ Mpc}^{-3}$ , which gives an integrated luminosity density of  $j = (2.02 \pm 0.15) \times 10^8 h L_\odot \text{ Mpc}^{-3}$ . From the total LF we extract the type-specific LFs based on measured *relative* type-specific LFs keeping the total luminosity density fixed. The type-specific LFs are required because the early-type and the late-type populations are dynamically different and contribute to the multiple imaging in distinctively different ways, namely that the early-type population contributes more to the total lensing rate and on average generates larger image splittings [4]. We use the relative LFs obtained from the Second Southern Sky Redshift Survey (SSRS2), which is based on 5404 local ( $z \leq 0.05$ ) galaxies. We obtain the following early-type ( $e$ ) and late-type ( $s$ ) LFs expressed in the  $b_J$  photometric system: for the early-type population,  $M_*^{(e)} - 5 \log_{10} h = -19.63_{-0.11}^{+0.10}$ ,  $\alpha^{(e)} = -1.00 \pm 0.09$ , and  $n_*^{(e)} = (0.64 \pm 0.19) \times 10^{-2} h^3 \text{ Mpc}^{-3}$ ; for the late-type population,  $\alpha^{(s)} = -1.22 \pm 0.02$ ,  $M_*^{(s)} = -19.69 \pm 0.04$ , and  $n_*^{(s)} = (1.20 \pm 0.11) \times 10^{-2} h^3 \text{ Mpc}^{-3}$ . To break a degeneracy we have chosen  $\alpha^{(s)} = \alpha$  and  $M_*^{(s)} = M_*$  since the total LF is dominated by late-type galaxies. For alternative type-specific LFs obtained from the 2dFGRS, the reader is referred to [4, 5]. When the alternative type-specific LFs are used, our derived limits on cosmological parameters are essentially unchanged.

The multiple imaging cross section of a galaxy can be related to and calculated from the line-of-sight velocity dispersion of the galaxy. However, the relation is not unique but depends on the mass profile and intrinsic shape of the galaxy. This dependence will be absorbed into a ‘‘dynamical normalization’’ factor  $\lambda(f)$  below. It is known that projected surface densities of the inner cylindrical regions of galaxies along the line-of-sight probed by gravitational lensing are well approximated by a singular isothermal mass profile or a profile similar to it [4]. In this Letter, we adopt a singular isothermal ellipsoid (SIE) as a galaxy lens model, whose projected density can be expressed in units of lensing critical surface density  $\Sigma_{\text{cr}} = c^2 D_{\text{OS}} / (4\pi G D_{\text{OL}} D_{\text{LS}})$  as

$$\kappa(x, y) = \frac{r_{\text{cr}}}{2} \frac{\sqrt{f} \lambda(f)}{\sqrt{x^2 + f^2 y^2}}, \quad (3)$$

where  $f$  is the apparent minor-to-major axis ratio,  $\lambda(f)$  is the dynamical normalization factor for a given dynamical

model, and

$$r_{\text{cr}} = 4\pi \left(\frac{\sigma}{c}\right)^2 \frac{D_{\text{OL}}D_{\text{LS}}}{D_{\text{OS}}} \quad (4)$$

is the critical radius for  $f = 1$ .  $D_{\text{OL}}$ ,  $D_{\text{LS}}$  and  $D_{\text{OS}}$  are angular diameter distances between observer (O), lensing galaxy (L), and source (S). Calculations of dynamical normalizations for axisymmetric cases (i.e. oblate and prolate) can be found in [4]. For the case of equal numbers of oblates and prolates,  $|\lambda(f) - 1| \lesssim 0.06$  for  $f > 0.4$ .

Let  $s_m(f)$  be the lensing cross section for image multiplicity  $m$  ( $= 2, 4$ ) due to the surface density given by equation (3) in units of  $r_{\text{cr}}^2$  (Eq. 4). Then, we have  $s_m(f) = [\lambda(f)]^2 \hat{s}_m(f)$  where  $\hat{s}_m(f)$  can be evaluated numerically [4]. The differential probability for a source with redshift  $z_s$  and flux density  $S$  to be multiply-imaged with image multiplicity  $m$  and image separation  $\Delta\theta$  to  $\Delta\theta + d(\Delta\theta)$ , due to a distribution of intervening galaxies of type  $g$  ( $g = e, s$ ) at  $z$  to  $z + dz$  modeled by SIEs and described by a type-specific Schechter LF, is given by

$$\begin{aligned} \frac{d^2 p_m^{(g)}}{dz d(\Delta\theta)} &= s_m(f) 8\pi^2 \gamma \left| c \frac{dt}{dz} \right| (1+z)^3 \left( \frac{D_{\text{OL}}D_{\text{LS}}}{D_{\text{OS}}} \right)^2 \\ &\times n_* \left( \frac{\sigma_*}{c} \right)^4 \frac{1}{\Delta\theta_*} \left( \frac{\Delta\theta}{\Delta\theta_*} \right)^{(\alpha\gamma + \gamma + 2)/2} \\ &\times \exp \left[ - \left( \frac{\Delta\theta}{\Delta\theta_*} \right)^{\gamma/2} \right] B_m(z_s, S), \end{aligned} \quad (5)$$

where  $B_m(z_s, S)$  is a magnification bias factor (i.e., an over-representation of multiply-imaged sources because of flux amplifications) which depends on a magnification probability distribution and  $|dN/dS|$  and can be calculated numerically [4]. In Eq. (5),  $\Delta\theta_*$  is a characteristic image (angular) separation given by

$$\Delta\theta_* = \lambda(f) 8\pi \frac{D_{\text{LS}}}{D_{\text{OS}}} \left( \frac{\sigma_*}{c} \right)^2. \quad (6)$$

The differential probability with  $\Delta\theta$  to  $\Delta\theta + d(\Delta\theta)$  can be obtained from Eq. (5):

$$\frac{dp_m^{(g)}}{d(\Delta\theta)} = \int_0^{z_s} \frac{d^2 p_m^{(g)}}{dz d(\Delta\theta)} dz. \quad (7)$$

The differential probability with any  $\Delta\theta > \Delta\theta_{\text{min}}$  due to galaxies at  $z$  to  $z + dz$  is given by

$$\begin{aligned} \frac{dp_m^{(g)}}{dz} &= s_m(f) 16\pi^2 \Gamma \left( \alpha + 1 + \frac{4}{\gamma} \right) \left| c \frac{dt}{dz} \right| (1+z)^3 \\ &\times n_* \left( \frac{\sigma_*}{c} \right)^4 \left( \frac{D_{\text{OL}}D_{\text{LS}}}{D_{\text{OS}}} \right)^2 B_m(z_s, S) \\ &- \int_0^{\Delta\theta_{\text{min}}} \frac{d^2 p_m^{(g)}}{dz d(\Delta\theta)} d(\Delta\theta). \end{aligned} \quad (8)$$

Finally, the integrated probability is given by

$$p_m^{(g)} = \int_0^{z_s} \frac{dp_m^{(g)}}{dz} dz. \quad (9)$$

For the sample of CLASS sources containing  $N_{\text{L}}$  multiply-imaged sources and  $N_{\text{U}}$  unlensed sources, the likelihood  $\mathcal{L}$  of observing the number and the properties of the multiply-imaged sources (Table 1) and the number of the unlensed sources given the statistical lensing model, is defined by

$$\ln \mathcal{L} = \sum_{i=1}^{N_{\text{U}}} \ln \left[ 1 - \sum_{m=2,4} p_m^{(\text{all})}(i) \right] + \sum_{k=1}^{N_{\text{L}}} \ln \delta p_m^{(\text{one})}(k), \quad (10)$$

where the integrated probability (Eq. 9)  $p_m^{(\text{all})}(i) = p_m^{(e)}(i) + p_m^{(s)}(i)$  and the differential probability (Eqs. 5, 7, or 8)  $\delta p_m^{(\text{one})}(k)$  is given by

$$\delta p_m^{(\text{one})}(k) = w^{(e)}(k) \delta p_m^{(e)}(k) + w^{(s)}(k) \delta p_m^{(s)}(k) \quad (11)$$

with  $w^{(e)}(k) + w^{(s)}(k) = 1$ . If the  $k$ -th lensing galaxy type is known to be an early-type (late-type),  $w^{(e)}(k) = 1$  ( $w^{(s)}(k) = 0$ ). If the  $k$ -th lensing galaxy type is unknown, we use  $w^{(g)}(k) = \delta p_m^{(g)}(k) / [\delta p_m^{(e)}(k) + \delta p_m^{(s)}(k)]$  if the lens redshift is known, and we use  $w^{(e)}(k) = 0.8$  and  $w^{(s)}(k) = 0.2$  otherwise. From Eq. (10), a “ $\chi^2$ ” is defined as

$$\chi^2 = -2 \ln \mathcal{L}. \quad (12)$$

We calculate the  $\chi^2$  (Eq. 12) over grids of the model free parameters (see below; in each grid point the  $\chi^2$  is minimized over the nuisance parameters) and determine the best-fit values and errors of the free parameters. We allow most of the critical parameters to be free while we fix the parameters that are well-determined by observations or to which the  $\chi^2$  is insensitive. The free parameters to be determined by minimizing the  $\chi^2$  are as follows: present matter density  $\Omega_m$ , present vacuum density  $\Omega_\Lambda$  or dark energy density  $\Omega_x$  (all expressed as fractions of the present critical density) with its constant equation of state  $w = p_x/\rho_x$  (where  $p_x$  and  $\rho_x$  are its isotropic pressure and uniform energy density), early-type and late-type characteristic velocity dispersions  $\sigma_*^{(e)}$  and  $\sigma_*^{(s)}$ , and the mean apparent axial ratio of galaxies  $\bar{f}$ . A critical but fixed parameter is the early-type characteristic number density  $n_*^{(e)}$ . However, whichever of the presently available choices of type-specific LFs we use, the derived constraints on cosmological parameters turn out to be virtually the same. One key assumption we make is that the (relatively) locally determined early-type number density  $n_*^{(e)}$  along with the faint-end slope  $\alpha^{(e)}$  have not evolved since  $z \sim 1$ . This appears to be a valid assumption based on current evidence and understanding [7]. However, if there is any significant reduction in the early-type number density at  $z \sim 0.6$  compared

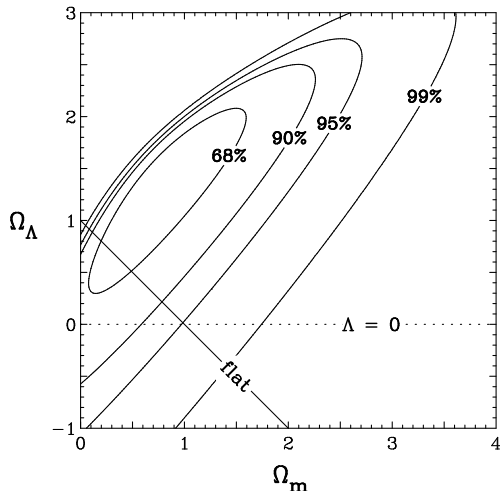


FIG. 1: Confidence limits in the  $\Omega_m$ - $\Omega_\Lambda$  plane.

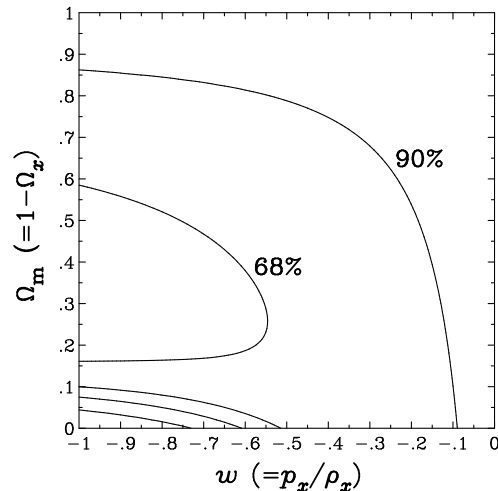


FIG. 2: Confidence limits in the  $w$ - $\Omega_m$  plane in flat cosmologies.

with the present epoch, our presently determined matter density (dark energy density) will be overestimated (underestimated).

We present our results based on the type-specific LFs derived using the SSRS2 LFs and a dynamical normalization assuming equal frequencies of oblates and prolates. Figure 1 shows likelihood regions in a matter plus vacuum cosmology: we find the combination  $\Omega_\Lambda - 1.2\Omega_m = 0.40^{+0.33}_{-0.56}$  (68%) ( $_{-1.57}^{+0.52}$  at 95%). Figure 2 shows the likelihood in the  $w$ - $\Omega_m$  plane with the prior that the universe is flat; we find  $w < -0.55^{+0.18}_{-0.11}$  (68%). This limit is in agreement with other recent results [8]. For a flat universe with a cosmological constant (i.e. for  $w = -1$ ), we find  $\Omega_m = 0.31^{+0.27}_{-0.14}$  (68%) ( $_{-0.23}^{+0.75}$  at 95%)  $_{-0.10}^{+0.12}$  (systematic). The identified systematics are due to the uncertainties in the redshift distribution and the differential number-flux density relation of the sources. For the flat  $w = -1$  case, other fitted values of the parameters are:  $\sigma_*^{(e)} = 198^{+53}_{-37}$  km s $^{-1}$ ,  $\sigma_*^{(s)} = 117^{+45}_{-31}$  km s $^{-1}$ , and  $\bar{f} < 0.83$ , all at 95%.

In conclusion, the likelihood function (or,  $\chi^2$ ; Eq. 12) of the CLASS data has well-defined confidence regions in the parameter space defined by our cosmological and galactic parameters. Our constraint in the  $\Omega_m$ - $\Omega_\Lambda$  plane based solely on lens statistics agrees with that from Type Ia supernovae observations [2]. Our determined value of  $\Omega_m$  in flat cosmologies is also in good agreement with several recent independent determinations [2]. Compared with previous works in lens statistics [4], our results imply not only positive but higher dark energy density. Therefore, our results, which are based on different physics, assumptions and astronomical relations, and independent sets of data, add to the evidence for a universe with low matter density and high dark-energy density.

- 
- [1] E.L. Turner, *Astrophys. J. Lett.*, **365**, L43 (1990); M. Fukugita and E.L. Turner, *Mon. Not. R. Astron. Soc.*, **253**, 99 (1991).
  - [2] See, e.g., A.G. Riess, et al., *Astron. J.*, **116**, 1009 (1998); S. Perlmutter, et al., 1999, *Astrophys. J.*, **517**, 565 (1999) (Type Ia Supernovae); A. Jaffe, et al., *Phys. Rev. Lett.*, **86**, 3475 (2001) (CMB); W.J. Percival, et al., *Mon. Not. R. Astron. Soc.*, **327**, 1297 (2001); astro-ph/0206256 (matter power spectra); S.M. Molnar, M. Birkinshaw and R.F. Mushotzky, *Astrophys. J.*, **570**, 1 (2002) (S-Z).
  - [3] S.T. Myers, et al., (to be published); I.W.A. Browne, et al., (to be published); For the distributions of sources in redshift and in flux density, see D.R. Marlow, et al., *Astron. J.*, **119**, 2629 (2000); J.P. McKean, et al., (to be published); I. Waddington, et al., *Mon. Not. R. Astron. Soc.*, **328**, 882 (2001); J.S. Dunlop, J.A. Peacock, *Mon. Not. R. Astron. Soc.*, **247**, 19 (1990).
  - [4] K.-H. Chae, (to be published) and references therein; in particular, P. Helbig, et al., *Astron. Astrophys. (Suppl.)*, **136**, 297 (1999) (a subsample of CLASS); C.S. Kochanek, *Astrophys. J.*, **466**, 638 (1996) (primarily optically-selected sample).
  - [5] For total LFs, see P. Norberg, et al., *Mon. Not. R. Astron. Soc.*, **328**, 64 (2002) (2dFGRS); M. Blanton, et al., *Astron. J.*, **121**, 2358 (2001); N. Yasuda, et al., *Astron. J.*, **122**, 1104 (2001) (SDSS). For type-specific LFs, see R.O. Marzke, et al., *Astrophys. J.*, **503**, 617 (1998) (SSRS2); D.S. Madgwick, et al., *Mon. Not. R. Astron. Soc.*, **333**, 133 (2002) (2dFGRS).
  - [6] G. de Vaucouleurs and D.W. Olson, *Astrophys. J.*, **256**, 346 (1982); M. Bernardi, et al., astro-ph/0110344 (SDSS) (Faber-Jackson); R.B. Tully and M.J. Pierce, *Astrophys. J.*, **533**, 744 (2000) (Tully-Fisher).
  - [7] See, e.g., P.J.E. Peebles, astro-ph/0201015, and references.
  - [8] See, e.g., S. Perlmutter, M.S. Turner, and M. White, *Phys. Rev. Lett.*, **83**, 670 (1999); R. Bean and A. Melchiorri, *Phys. Rev. D.*, **65**, 041302 (2002).